CRB-based comparative study of array signal processing direction finding methods supported with SDR platform implementation

CRB-based comparative study of array signal processing direction finding methods supported with SDR platform implementation

O A Elkasrawi[1], A M Abdelaziz[2], H E AbouBakr[1] and M A Aboelazm[1]

[1]Department of Electronic Warfare, Military Technical College, Kobry ELkobba, Cairo,Egypt.
[2]Department of Communication, Military Technical College, Kobry ELkobba, Cairo,Egypt.

E-mail: osama.elkasrawi@gmail.com

Abstract. Radio Direction-Finding (DF) is an extremely important process in numerous commercial and military applications. Array signal processing-based DF methods have been developed to improve estimation performance in recent applications that require higher resolution and accuracy. Practically, angle of arrival (AOA) estimation is challenging due to various intrinsic and extrinsic parameters that affect the results. Therefore, clarifying these parameters and researching their impact on various DF methods are considered important research topics. The Cramer-Rao Bound (CRB) for estimating AOA is calculated based on a model of a linear antenna array system. This bound identify the factors that significantly impact the estimation performance. The current study conducts a comparative analysis of the most widely used array-signal-processing-based direction-finding (DF) methods under different conditions of the CRB parameters. According to the simulation results, Multiple Signal Classification (MUSIC) AOA estimator provides more accurate and stable results. Accordingly, it is chosen for implementation using a prototype testbed based on Software Defined Radio (SDR) technology using National Instruments Universal Software Radio Peripheral (NI-USRP) platform version 2930. Experimental outcomes were tested at various AOA values. The appendix includes the complete derivation for the CRB relation applied on the system model.

1. Introduction

Direction-Finding (DF) has drawn significant attention in the field of array signal processing as it is used in numerous applications, both military and civilian, including radar, navigation, tracking RF sources, rescue, wireless communications, emergency assistance cases, radio astronomy, army surveillance, and security services [1–4]. Observing and determining the directions of the incoming signals on the antenna array is the foundation of the radio monitoring systems. To estimate the AOA of incoming waves, many different methods have been developed over time.

- Classical DF methods
  - (i) DF based on directional antennas: This setup is simple and inexpensive, and it uses a mechanical rotated directional antenna to provide great sensitivity, making it the simplest method of DF. Due to the antenna's limited rotation speed and directivity, this approach has some drawbacks that reduce the probability of intercept [1].
  - (ii) DF based on Watson-watt method: It has a compact size and a straightforward implementation. However, this method has poor accuracy that can not handle numerous sources simultaneously and have not accurate correct measurements in multi-path situations [5, 6].

(iii) DF based on Doppler effect: It operates in both stationary and moving modes, however it is unable to handle correlated sources. Moreover,it performs poorly with signals that are horizontally polarised and since Pseudo-Doppler requires greater sensitivity, the receiving circuit quality needs to be more sophisticated. [1, 6].

(iv) DF based on Correlative Interferometer (CI): compared to previous DF methods, CI has many important advantages. It has excellent accuracy, great multi-path immunity, and the accuracy of CI-based systems is not impacted by signal polarization. There are some operational constrains that appear on inability to handle multiple sources of the same frequency, having poorer resolution and accuracy than super-resolution methods and requiring very specialized engineering and production resources due to the related extremely strict design and manufacturing tolerances [1, 7–9].

- Array-signal-processing-based DF methods: These methods use propagation delays between antenna array elements to calculate the signal's AOA [5, 8, 10, 11]. With benefits like Array Gain, handling many signals simultaneously, and interference reduction, these methods significantly outperform classical DF methods in terms of estimation performance and resolution [8, 9, 12]. the following methods represents some of the most applicable methods of this category.

  (i) DF based on Bartlett method: It is seen to be the most straightforward technique, although it lacks good resolution and precision [3, 10, 11, 13].

  (ii) DF based on Capon method: Although it outperforms Bartlett, it does not offer the highest estimation accuracy or resolution [2, 10, 11, 13].

  (iii) DF based on Linear Prediction: This approach is based on predicting the output of a single element utilizing linear combinations of other elements' outputs, and then getting array weights that minimize the mean-square-error between both estimated and real output. However, the choice of that element influences the estimating performance and the resolution capability, there is no standard for choosing the position of the selected element and this consider a drawback which limits its practical implementation [3, 10, 11].

  (iv) DF based on Maximum Entropy: Although it is viewed as a development of beamforming techniques that produces improved performance, its resolution and performance are inferior to those of sub-space decomposition techniques. This approach requires choosing a specific column of the inverse array correlation matrix in order to compute the spatial spectrum. It is important to note that the selection of which column from the inverse array correlation matrix to employ might have a big impact on the reached resolution [3, 10, 11].

  (v) DF based on MUSIC algorithm: Although it is more reliable and provides a high level of resolution and accuracy, it cannot resolve highly correlated sources without a pre-processing stage and it must know exactly how many incoming signals there are [2, 10, 12–15].

  (vi) DF based on Root-MUSIC algorithm : It is regarded as a modified form of the MUSIC algorithm. It minimizes computational complexity and raises estimation resolution. Its limitation to uniform-linear-array (ULA) is a vital drawback [2, 4, 10, 13, 15].

  (vii) DF based on ESPRIT algorithm: Although it reduces computing complexity, it can't handle correlated sources and requires a doublets array [2, 11, 13, 14].

Despite of the benefits that array-signal-processing-based DF methods have, a serious drawback exists in their computational intensive needs [2, 8]. The CRB-based study depends on the concept that utilizing noisy data to estimate parameters will produce inaccurate results [16]. This indicates that there is an estimation variance between the actual value and the estimated value in every estimating process. In real-time applications, numerous variables, including those linked to the application environment as well as the source of the incoming signal, influence the outcomes of a AOA estimation process such as signal-to-noise ratio (SNR), number of the received snapshots, total number of elements in the array, coherence between received signals, the value of the AOA itself, ... etc [4, 12, 17, 18]. The CRB derived equation of the system under study can serve to clarify these parameters, and analyzing these parameters can then aid to reduce the estimation variance and enhance estimation performance [19, 20].

In this paper, we study the key parameters affecting AOA estimation process which are specified from the derived CRB equation applied on linear antenna array DF system. In addition, a comparison study based on these parameters is used to select the appropriate DF method to be implemented using SDR technology.

The remainder of this paper is structured as follows, Section "2" presents the system modeling and its CRB derived equation to define the parameters that affect the estimation performance. The key benefits and drawbacks of the DF methods under study and their fundamental operating principles are outlined in section "3". Section "4" provides the simulation analysis,which supports the conclusion of the theoretical analysis. Moreover,the estimation performance of the most popular DF methods is compared under various conditions of the parameters affecting them. The experimental implementation of the most appropriate and efficient DF method is included in section "5" using a NI-USRP SDR platform. Section "6" then concludes the paper research work. Finally, "Appendix A" contains the detailed mathematical derivation for the CRB of the system under consideration.

2. System modelling and CRB derivation

2.1. System modelling

As shown in figure 1, consider a far-field narrow band Signal-Of-Interest (SOI) incident on a ULA composed of M isotropic antenna elements with an inter-element spacing of d. The SOI is assumed to be impinging with center-frequency F_c and angle θ. Suppose we are coping with a White-Gaussian-Noise channel (AWGN) in which noise samples are i.i.d and $\sim \mathcal{N}(0,\, \sigma^2)$ where σ^2 is the noise variance.

The received signal can be expressed as follows

$$\mathbf{X} = \mathbf{a}(\theta)\mathbf{s} + \mathbf{N} \tag{1}$$

where, $\mathbf{N} \in \mathcal{C}^{M\times J}$, $\mathbf{s} \in \mathcal{C}^{1\times J}$ and J are the noise matrix, the vector of SOI samples and the total number-of-snapshots, respectively. Steering vector $\mathbf{a}(\theta) \in \mathcal{C}^{M\times 1}$ is defined as follows

$$\mathbf{a}(\theta) = [1\ e^{-i2\pi F_c \frac{(m-1)d\sin(\theta)}{C}}\ \ldots\ e^{-i2\pi F_c \frac{(M-1)d\sin(\theta)}{C}}]^T \tag{2}$$

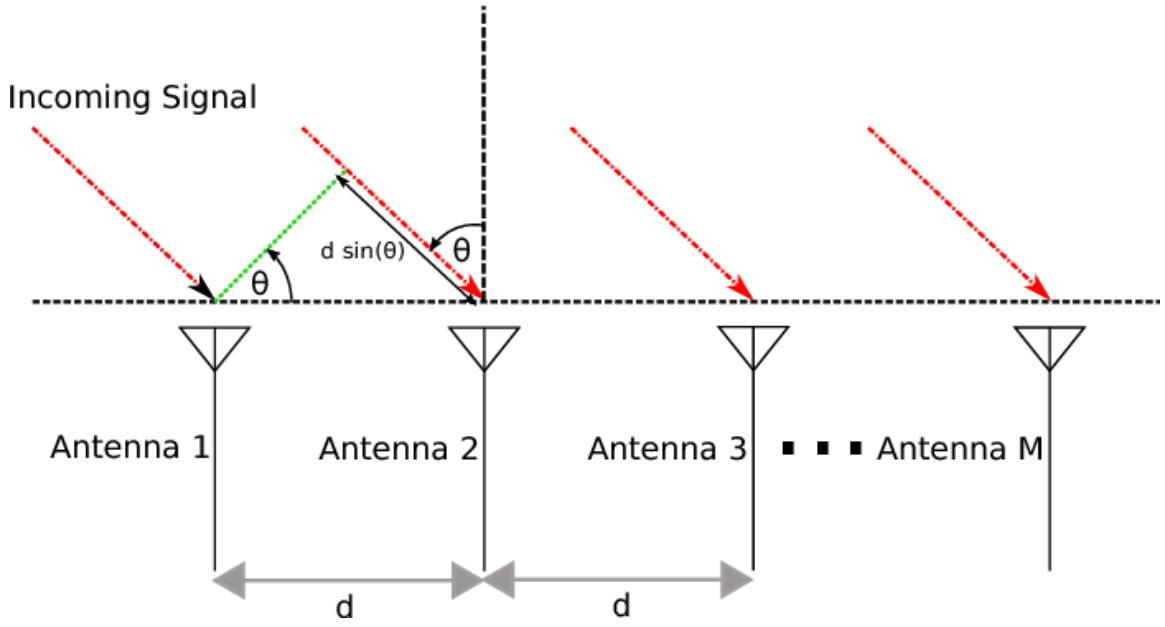

Figure 1. System Model.

where θ is AOA of SOI, $d = \lambda/2$ and λ represents the wavelength related to F_c. DF algorithms based on array processing depend on array recieved signal correlation matrix, which is defined as follows

$$\mathbf{R} = \mathbb{E}[\mathbf{X}\mathbf{X}^H] \tag{3}$$

As previously assumed, SOI and noise are uncorrelated, so equation (3) can be reduced to the following form

$$\mathbf{R} = \mathbf{a}(\theta)\mathbb{E}[\mathbf{s}\mathbf{s}^H]\mathbf{a}^{\mathbf{H}}(\theta) + \mathbb{E}[\mathbf{N}\mathbf{N}^H] \tag{4}$$

$$= \mathbf{a}(\theta)\mathbf{R}_{\mathbf{ss}}\mathbf{a}^{\mathbf{H}}(\theta) + \sigma^2\mathbf{I}_{M\times M} \tag{5}$$

$$= \mathbf{a}(\theta)\mathbf{R}_{\mathbf{ss}}\mathbf{a}^{\mathbf{H}}(\theta) + \mathbf{R}_{\mathbf{nn}} \tag{6}$$

where $\mathbf{R_{nn}}$ and $\mathbf{R_{ss}}$ represent the noise and the source correlation matrix, respectively.

Practically, during reception time, receiver can acquire a finite number of snapshots, just J snapshots, hence correlation matrix can be written as follows [3, 14]

$$\hat{\mathbf{R}} = \frac{1}{J}\sum_{j=1}^{J}\mathbf{X}\mathbf{X}^H \tag{7}$$

2.2. CRB derivation

In real-time applications, the SOI that impinges on the array usually has unknown amplitude and direction, as well as low SNR and is exposed to other practical issues [4, 12, 15]. As a result, AOA estimation is considered to be a challenging problem. Therefore, determining the factors that have an impact on the AOA estimation procedure is crucial aspect. The minimum estimate variance for a particular system under consideration is provided by CRB, which warns that parameter estimation using noisy data will produce noisy estimates [16]. The system under study's CRB equation can be derived to help clarify these parameters [19, 20]. Consequently, analyzing these parameters can help to lower the estimation variance and improve estimation performance. For the system modeled in Section "2.1", the CRB equation can be defined as follows

$$CRB \geq \frac{1}{2J\alpha(Kd\cos(\theta))^2\sum_{m=1}^{M}(m-1)^2} \tag{8}$$

Depending on equation (8), the AOA estimation process can be influenced by several factors, such as the number of snapshots, number of array elements, SNR, value of the AOA itself,inter-element spacing, SOI carrier frequency and its bandwidth. The impact of some of these parameters on AOA estimation performance will be discussed in Section "4". The derivation of equation (8) has been explained in detail in "Appendix A".

3. DF algorithms based on array signal processing

3.1. Beam-forming for spectral estimation

The basic principle of BF methods is to steer the antenna array in one direction at a time and measure the total Received Signal Strength (RSS) to have the maximum signal's power at the correct AOA.

3.1.1. DF based on Bartlett method. It calculates the signal power at each possible AOA, the true AOA is selected according to the highest power value in the spectrum.

This process is similar to array mechanical steering and measuring received power at each possible direction unless the steering occur electronically by introducing specific delays / weights, it sometimes called delay and sum method, on the received signal of every array element. In this method, the maximum received power occurs at the true AOA. Pseudo-spectra of Bartlett method can be written as [2, 13]

$$P_{Bar}(\theta) = \frac{\mathbf{a}^H(\theta)\mathbf{R}\mathbf{a}(\theta)}{N^2} \tag{9}$$

Despite being computationally simpler, Bartlett method suffers from poor resolution and this reduces its performance and effectiveness as the ability to resolve angles is limited by the array Half-Power Beam-Width (HPBW),which has an inverse proportional relation with the number of array elements so an increase in resolution requires a larger array [2, 10].

For large array lengths with inter-element spacing, $d{=}\lambda/2$, the AOA resolution value is approximately $1/M$,which approximately equals to HPBW [10].

3.1.2. DF based on Capon method. It is similar to the Bartlett method, since it evaluates the power of the received signal in all possible directions. In this method, the mean output received power is minimized in order to minimize the contributed power from undesired signals in the undesired directions and also to minimize noise power while keeping unity response in the direction of interest. Pseudo-spectra of Capon method can be written as [2]

$$P_{Cap}(\theta) = \frac{1}{\mathbf{a}^H(\theta)\mathbf{R}^{-1}\mathbf{a}(\theta)} \tag{10}$$

This method has a disadvantage of the computation of the inverse matrix,which leads to have a poor performance for the case of highly correlated signals [4]. This method has better resolution than Bartlett method but it does not has the best resolution w.r.t. all methods [11, 13].

3.2. DF based on sub-space decomposition algorithms

These algorithms are considered high-resolution algorithms and they are known as subspace decomposition algorithms because they depend on decomposing the correlation matrix according to the following considerations [11]

- The space spanned by eigen-vectors of the correlation matrix can be decomposed into two orthogonal sub-spaces: signal subspace and noise subspace.
- Steering vectors associated with signals of interest are orthogonal to noise subspace and contained in signal subspace.
- Noise subspace is spanned by eigen-vectors with smallest eigen-values and on the contrary signal subspace is spanned by eigen-vectors with the largest eigen-values.

Therefore, these algorithms search for directions that have steering vectors, which are orthogonal to noise-subspace and contained in signal-subspace [11].

3.2.1. DF based on MUSIC algorithm. this algorithm depends on the orthogonality between the signal or noise subspaces supposing that the noise in the receiving channels is uncorrelated with SOIs. The steering vector corresponding to SOI, $\mathbf{a}(\theta)$, and this implies $\mathbf{a}(\theta) * \mathbf{Q}_n = 0$, where $\mathbf{Q}_n$ is the matrix corresponding to noise subspace and its columns contain eigen-vectors that correspond to the smallest eigen-values. In a practical situation, $\mathbf{a}(\theta)$ and $\mathbf{Q}_n$ will not be precisely orthogonal. The following equation is known as MUSIC pseudo-spectrum and it gives a very large value when θ equal to AOA of the corresponding SOI [2, 11, 13].

$$P_{MUS}(\theta) = \frac{1}{\mathbf{a}^H(\theta)\mathbf{Q}_n\mathbf{Q}_n^H\mathbf{a}(\theta)} \tag{11}$$

When signals are highly correlated, traditional MUSIC is not accurate in its estimation, and therefore, a spatial-smoothing-technique-based pre-processing method is necessary to address this scenario [13]. MUSIC algorithm also is constrained to the precise knowledge of the number of incoming signals [11].

3.2.2. DF based on Root-MUSIC algorithm. The basic idea of this algorithm is represented in the straightforward AOA estimation through the search for specific polynomial zeros. The pseudo-spectrum of MUSIC algorithm becomes equal to that polynomial on the unit circle, and MUSIC-spectrum peaks, that represent the estimated AOAs, exist as the roots that existed close to the unit circle [13]. This algorithm provides enhanced resolution and a lower computational complexity but it is limited to ULA architecture [2, 14]. After calculating the steering vectors by ULA and estimating the correlation matrix, MUSIC pseudo-spectrum represented in equation (11) will be simplified to the following expression

$$P_{RMUS}(\theta) = \frac{1}{\mathbf{a}^H(\theta)\mathbf{B}\mathbf{a}(\theta)} \tag{12}$$

where $\mathbf{B} = \mathbf{Q}_n\mathbf{Q}_n^H$. Hence, denominator of equation (12) can be written as follows

$$\begin{aligned}\mathbf{a}^H(\theta)\mathbf{B}\mathbf{a}(\theta) &= \sum_{m=1}^{M}\sum_{n=1}^{M} e^{i2\pi\frac{(m-1)d\sin(\theta)}{\lambda}} b_{mn} e^{-i2\pi\frac{(n-1)d\sin(\theta)}{\lambda}} \\ &= \sum_{l=-M+1}^{M-1} b_l e^{-i2\pi\frac{ld\sin(\theta)}{\lambda}}\end{aligned} \tag{13}$$

where b_{mn} is the element of the m^{th} row and n^{th} column of $\mathbf{B}$ and b_l is sum of l^{th} diagonal elements of $\mathbf{B}$ and can be defined as follows

$$b_l = \sum_{n-m=l} b_{mn} \tag{14}$$

Simplifying equation (13) as follows

$$E(z) = \sum_{l=-M+1}^{M-1} b_l z^l \tag{15}$$

where $z = e^{-i2\pi\frac{d\sin(\theta)}{\lambda}}$.

Roots of equation (15) that closest to unit circle represents the MUSIC pseudo-spectrum pole and can be expressed in polar form as follows

$$z_v = |z_v|e^{iarg(z_v)}, v = 1, 2, ..., 2(M-1) \tag{16}$$

where $arg(z_v)$ represents the phase of the root z_v. Hence, the AOA can be calculated from the following equation

$$\theta_v = -\arcsin\left(\frac{\lambda}{2\pi d} arg(z_v)\right) \tag{17}$$

3.2.3. DF based on ESPRIT algorithm. ESPRIT algorithm symbolizes Estimation of Signal Parameters through Rotational Invariance. This algorithm estimates the AOA directly without the calculation of a pseudo-spectrum, nor even the search for roots of the Root-MUSIC polynomial [14]. As illustrated in figure 2, this algorithm decomposes the main array into two sub-arrays of similar antennas such that One sub-array can be got by a translation of the other [10, 13]. Although the ESPRIT algorithm has a reduced computing complexity, it needs a doublets array and cannot handle correlated sources [11].

Getting the observation vectors $x_1(t)$ and $x_2(t)$ of the two subarrays, the received signal can be modeled as follows

$$\begin{aligned}\mathbf{x}(t) &= \begin{bmatrix}\mathbf{x_1}(t) \\ \mathbf{x_1}(t)\end{bmatrix} \\ &= \begin{bmatrix}\mathbf{A_1} \\ \mathbf{A_1}\Phi\end{bmatrix}\mathbf{s(t)} + \mathbf{n(t)}\end{aligned} \tag{18}$$

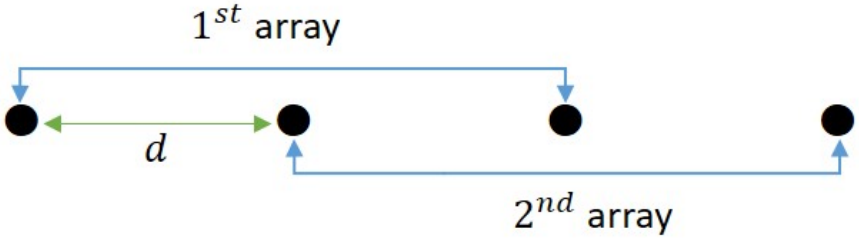

Figure 2. Array configuration for ESPRIT algorithm.

where $\Phi = diag\left[e^{i\frac{2\pi}{\lambda}\sinh\theta_1}, ..., e^{i\frac{2\pi}{\lambda}\sinh\theta_v}, ..., e^{i\frac{2\pi}{\lambda}\sinh\theta_D}\right]$, $v = 1, 2, ..., D$, D is the number of incident SOI and A

The correlation matrix can be described as follows

$$\begin{aligned}\mathbf{R_{xx}} &= \begin{bmatrix}\mathbf{R_{11}}\\ \mathbf{R_{22}}\end{bmatrix}\\ &= \begin{bmatrix}\mathbf{A_1}\\ \mathbf{A_1}\Phi\end{bmatrix}\mathbf{R_{ss}}\begin{bmatrix}\mathbf{A_1^H} & \Phi^H\mathbf{A_1}^H\end{bmatrix} + \sigma^2\mathbf{I}\end{aligned} \tag{19}$$

By applying Eigen-decomposition on the Correlation matrix represented in equation (19), these results will be

- M eigen-values with D largest eigen-values are correspond to the D sources
- There exist a matrix $\mathbf{Q_s}$ of dimension MXD which contains the eigen-vectors corresponding to the signal sub-space.
- Signal sub-space, formed by the whole array, can be divided into two sub-spaces $\mathbf{Q_{s1}}$ and $\mathbf{Q_{s2}}$ corresponding to the first and the second sub-array, respectively.
- $\mathbf{Q_{s1}}$ and $\mathbf{Q_{s2}}$ columns contains eigen-vectors that related to the eigenvalues of correlation matrix of the two sub-arrays.

The relation between $\mathbf{Q_{s1}}$ and $\mathbf{Q_{s2}}$ can modelled as follows

$$\mathbf{Q_s} = \begin{bmatrix}\mathbf{Q_{s1}}\\ \mathbf{Q_{s2}}\end{bmatrix} = \begin{bmatrix}\mathbf{A_1T}\\ \mathbf{A_1\Phi T}\end{bmatrix} \tag{20}$$

Since the sub-arrays are translationally related to each other, the signal sub-spaces corresponding to them are related by unique transformation matrix Ψ and equation (20) can be written as

$$\begin{aligned}\mathbf{Q_{s2}} &= \mathbf{Q_{s1}}\Psi = \mathbf{A_1\Phi T}\\ &= \mathbf{A_1TT^{-1}\Phi T}\end{aligned} \tag{21}$$

Consequently, Ψ can be written as

$$\Psi = \mathbf{T^{-1}\Phi T} \tag{22}$$

The eigen-values of Ψ correspond to the diagonal elements of Φ. Therefore, using these eigen-values, the AOA can be estimated as follows

$$\theta_v = \arcsin\left(\frac{\lambda}{2\pi d}arg(e_v)\right) \tag{23}$$

where v=1,2, ... , D and $e_1, e_2, ..., e_D$ represent eigen-values of Ψ.

4. Simulation analysis

In order to evaluate the performance of the AOA estimation algorithms, previously discussed in section 3, simulation analysis using MATLAB is performed. In this simulation, two uncorrelated narrow-band SOIs with AOAs of $\theta_1 = -5°$ and $\theta_2 = 5°$, respectively, incident on ULA consisting of M elements with inter-element spacing of $d = \frac{\lambda}{2}$. Additionally, it is assumed that J snapshots will be taken over AWGN propagation channel.

The performance analysis is based on RMSE calculation as a function of SNR, total number of snapshots and the number of elements in the array [13]. The results are averaged over 100 independent test runs. RMSE of the estimated AOA can be described as follows

$$RMSE = \sqrt{\frac{1}{100Z}\sum_{r=1}^{100}\sum_{b=1}^{Z}(\hat{\theta}_b(r) - \theta_b)^2} \tag{24}$$

where $\hat{\theta}_b(r)$ is the estimate of actual θ_b at the r^{th} run and Z is the total number of the signals impinged on the array.

4.1. The effect of varying the number-of-array-elements

In this simulation, the number of array elements varies with values $[4, 6, 8, 10, 12, 14, 16]$ at SNR $= 10dB$ and $J = 500$ snapshot.

According to figure 3, it is observed that increasing array elements tends to decrease RMSE and hence improves estimation performance, but at the expense of raising computation complexity and slowing down processing speed. In practical applications, it is necessary choosing an appropriate number of array elements to guarantee adequate estimation performance and speed up processing. As seen in figure

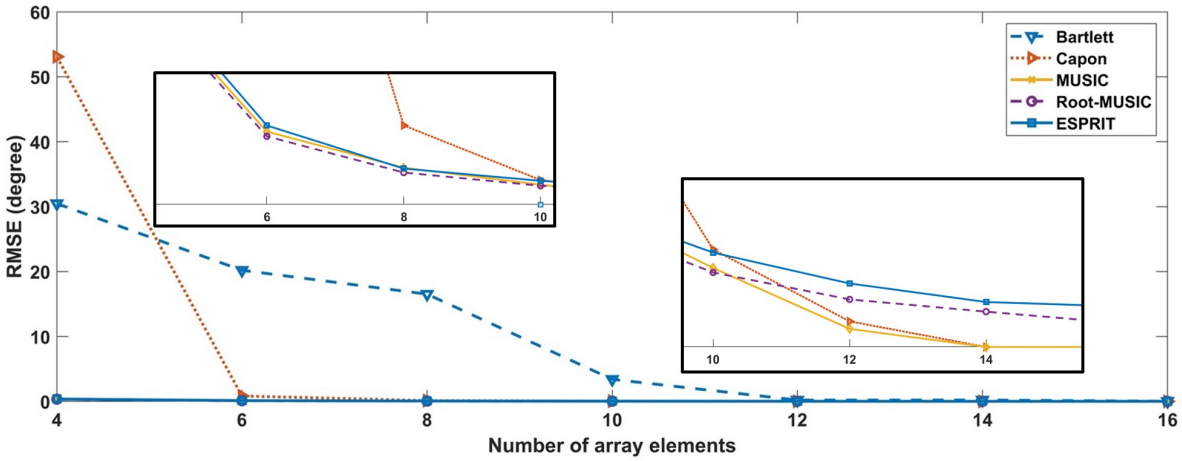

Figure 3. RMSE Vs number of elements.

3, Capon and Bartlett methods give the worst results compared to the other algorithms. Additionally, as shown in figure 3, simulation results indicate that Root-MUSIC, ESPRIT, and MUSIC achieve equivalent performance when M is smaller than 10. It is clear that MUSIC algorithm starts to have the best estimation performance when M is more than 10 elements, with its RMSE decreasing to zero when M is more than 14 elements.

4.2. The effect of varying total number of snapshots

In this simulation, total number of snapshots varies with values $[100, 200, 300, ..., 1000]$ at SNR $= 10dB$ and $M = 10$ elements.

As shown in figure 4, increasing the number of snapshots decreases RMSE and hence improves estimation performance, but at the expense of raising computation complexity and slowing down processing speed. In practical applications, it is necessary to choose an appropriate number of snapshots to guarantee adequate estimation performance and speed up processing.

As shown in figure 4, Bartlett method gives the worst results compared to the other algorithms. Additionally, Capon method achieves a better estimation performance but not the best of all.

As shown in figure 4, When there are fewer than 100 snapshots, the ESPRIT method outperforms other algorithms in terms of estimation performance. Simulation results of Root-MUSIC and MUSIC algorithms achieve equivalent performance when there are more than 100 snapshots, and they outperform other algorithms with their RMSE decrease below 0.05 degree when there are more than 300 snapshots.

4.3. The effect of varying SNR

In this simulation, SNR ,in decibels, varies with values $[-10, -5, 0, 5, ..., 30]$, with $J = 500$ snapshot and $M = 10$ elements. As shown in figure 5, increasing the SNR often lowers RMSE and hence improves estimation performance. Capon and Bartlett methods give the worst results compared to the

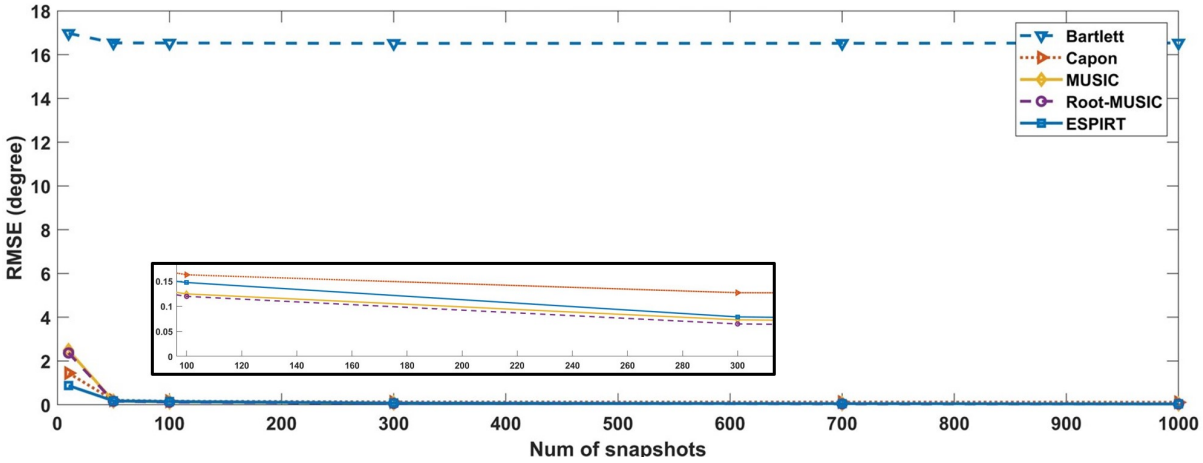

Figure 4. RMSE Vs number of snapshots.

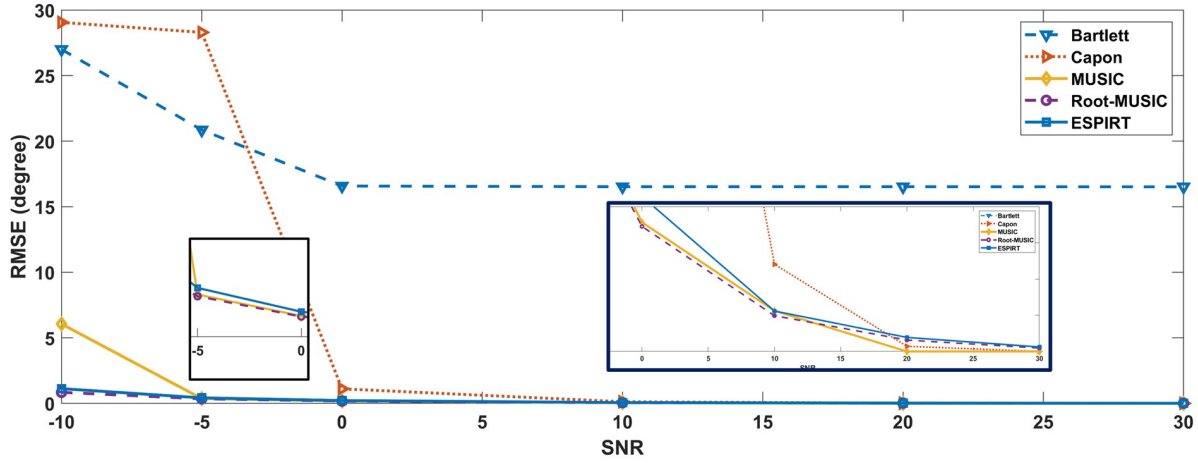

Figure 5. RMSE Vs SNR.

other algorithms, as seen in figure 5.

For SNR values between -10 and -5 dB, the Root-MUSIC and ESPRIT algorithms outperform other algorithms in terms of estimation performance. As shown in figure 5, the Root-MUSIC and MUSIC algorithms achieve equivalent performance at SNR values between -5 and 10 dB. When SNR equals more than 10 dB, the MUSIC algorithm begins to outperform other algorithms and has the best estimation performance. At SNR = 10 dB, RMSE of MUSIC algorithm decreases to almost 0.05 degree, and at SN = 20 dB and above, it decreases to 0 degree. Consequently, one of the main areas of study for high-resolution DF continues to be an open area of research for improving AOA estimation performance in low SNR scenarios.

5. Experimental results

According to simulation analysis and theoretical study, MUSIC algorithm is widely used for its accuracy and robustness, moreover, it is appropriate for being used in the experimental implementation. In table 1, the hardware components utilized in this experiment are listed in detail. Figure 6 illustrates the block-

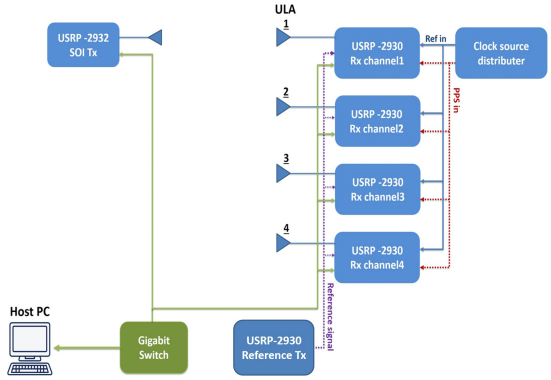

Figure 6. DF experiment block-diagram.

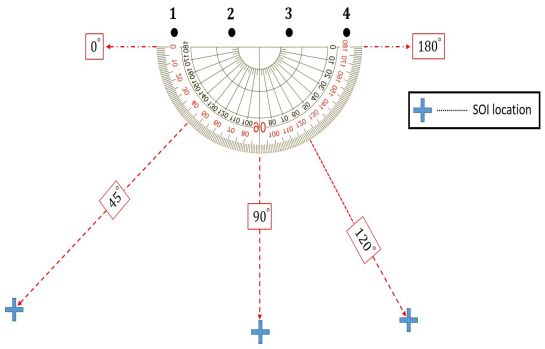

Figure 7. AOA measurement scalling.

diagram of DF experiment setup in which four USRPs-2930 constitute a four-channel RF receiver and another one is used as an SOI transmitter. An external clock distributor (Octoclock) is used to synchronize the local-oscillator (LO) by connecting a 10MHz reference clock to the Ref-in port in Rx-USRPs. In addition, this reference clock is also used to align the ADC's timestamp by connecting the 1PPS signal generated by the Octoclock to the PPs-in port in Rx-USRPs. GPSDO must be manually disconnected in all used-USRPs in order to accept external reference input signals.

Another USRP-2930 is used to perform calibration process to cancel out the constant relative phase offsets that exist between receiving channels by using a deterministic reference signal (ref-sig) that is duplicated by the four-port RF power splitter. The power splitter output signals are then fed directly into each $RX2$ port in each USRP. Four antennas are attached to each RX1/TX1 port in each USRP to capture SOI.

According to the prior description, the receiver acquires two signals, ref-sig and the SOI. A digital filter is used to separate these signals. At first, ref-sig is separated and utilized to estimate the phase offsets between reception paths. Secondly, SOI is also separated and calibrated using these estimated phase offsets before applying the MUSIC algorithm. Figure 7 represents the AOA measurement scalling [21]. A radio transmitter, operated as an SOI, is configured to generate an unmodulated sine-wave with a center frequency of 920 MHz. For acquiring the SOI, receiver channels are tuned with the same center frequency. The antenna array has an inter-element spacing of 16.3 cm, which equals nearly half the wavelength. The SOI has a base-band frequency of 100 kHz and the ref-sig has the same center frequency with a base-band frequency of 10 kHz. Measurements were taken with the target source placed at different AOAs

Table 1. List of used components in experment setup.

Item	Version	Amount	Function
CPU	HP Core I7	1	Host for signal processing
USRP	NI USRP-2930	6	4 USRPs to form 4-channel receiver (Rx),1 utilized as reference-signal transmitter and 1 utilized as SOI transmitter
Clock distributor	OctoClock-G CDA-2990	1	LO synchronization in all Rx-USRPs and Aligning ADC timestamp
Gigabit Ethernet Switch	TP-Link	1	Connect all USRPs to host PC
Software	LabVIEW 2019		Processing environment
Rf antennas	VERT400 Antenna 783074-01	5	4 antennas for the receiver and one for SOI transmitter
Operating system	Windows 10		
power splitter	Mini-Circuits ZFRSC-4-842-S+	1	power splitting for the calibration process
Cables	SMA-M to SMA-M	17	For all connections illustrated in fig 6

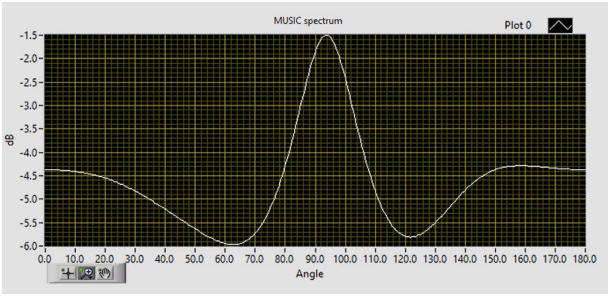

Figure 8. AOA estimation for SOI located at 90°.

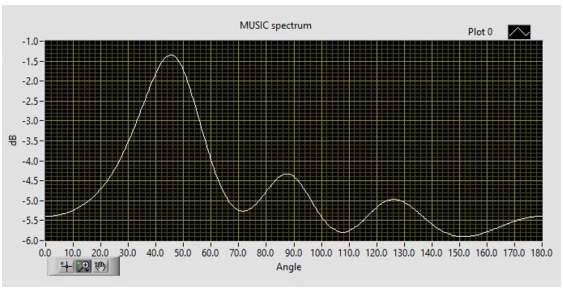

Figure 9. AOA estimation for SOI located at 45°.

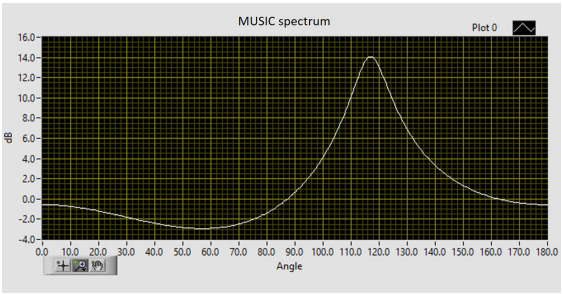

Figure 10. AOA estimation for SOI located at 120°.

according to the measurement scaling as shown in [21]. In table 2, the difference between the correct and estimated angles for different cases of AOA is depicted.

Figures 8, 9 and 10 represent the MUSIC pseudo-spectrum, $P_{MUS}(\theta)$, computed according to equation (11), for $\theta = 90°, 45°$ and $120°$. The maximum pseudo-spectrum value represents the estimated values of AOAs.

6. Conclusion

At first, the CRB for AOA estimation process is derived to identify the factors affecting the estimation process. Subsequently, various DF algorithms are studied.

Theoretical study ensures that Bartlett method is regarded as one of the simplest ones but it doesn't provide good resolution and accuracy. Capon method is better than Bartlett method but it doesn't provide the best estimation accuracy and resolution. MUSIC algorithm is one of the common super-resolution DF method and it is considered to be more stable and provides high resolution in AOA estimation.

Table 2. Experimental results.

True AOA	Estimated AOA	Error Ratio
90°	93.5°	3.8%
45°	45.5°	1.11%
120°	117°	2.5%

MUSIC algorithm constrains precise knowledge of the number of incoming signals and has a limitation in resolving correlated sources. Root-MUSIC algorithm is deemed a modified version of MUSIC algorithm to improve estimation resolution and reduce computational complexity but it has the limitation of applying only to ULA. ESPRIT algorithm achieves a lower computational complexity but it can't deal with correlated sources, where it needs doublets array.

In simulation analysis, DF algorithms are compared according to the parameters appeared in CRB equation. According to simulation results, subspace decomposition-based DF algorithms enhance estimation accuracy and resolution more than spectral estimation-based algorithms.

The overall performance analysis between DF algorithms based on array processing yields in giving the best rating for MUSIC algorithm because of its robustness and higher accuracy and resolution. Consequently, MUSIC algorithm is selected to be implemented on SDR platform, USRP, which is programmed by LABVIEW. Tests were taken with the SOI placed at different AOAs.

Our future work will focus on improving estimation performance and resolution for MUSIC-based Direction finders in low SNR environments and in the presence of correlated sources.

Appendix A. CRB derivation

Depending on the modeled system in Section "2.1", CRB for AOA estimation using ULA is derived. We begin with deriving Conditional-Probability-Density-Function (CPDF). From equation (1) the CPDF is derived as follows

$$P(\mathbf{X}/\theta) = const * e^{-(\frac{(\mathbf{X}-\mathbf{a}(\theta)\mathbf{s})^H(\mathbf{X}-\mathbf{a}(\theta)\mathbf{s})}{\sigma^2})} \tag{A.1}$$

where (const) represents a constant term.

$$\begin{aligned} P(\mathbf{X}/\theta) &= \prod_{l=1}^{J} const * e^{-(\frac{(\vec{x}_l-\mathbf{a}(\theta)s_l)^H(\vec{x}_l-\mathbf{a}(\theta)s_l)}{\sigma^2})} \\ &= (\prod_{l=1}^{J} const) * e^{-\frac{1}{\sigma^2}\sum_{l=1}^{J}(\vec{x}_l-\mathbf{a}(\theta)s_l)^H(\vec{x}_l-\mathbf{a}(\theta)s_l)} \\ &= (const) * e^{-\frac{1}{\sigma^2}\sum_{l=1}^{J}(\vec{x}_l-\mathbf{a}(\theta)s_l)^H(\vec{x}_l-\mathbf{a}(\theta)s_l)} \end{aligned} \tag{A.2}$$

Equation (A.2) can be represented in logarithmic form as follows

$$\begin{aligned} \ln P(\mathbf{X}/\theta) &= \ln const + \frac{-1}{\sigma^2}\left(\sum_{l=1}^{J}(\vec{x}_l - \mathbf{a}(\theta)s_l)^H(\vec{x}_l - \mathbf{a}(\theta)s_l)\right) \\ &= const + \frac{1}{\sigma^2}\sum_{l=1}^{J}[-(\vec{x}_l^H\vec{x}_l) - \big((\mathbf{a}(\theta)s_l)^H\mathbf{a}(\theta)s_l\big) + \vec{x}_l^H(\mathbf{a}(\theta)s_l) + (\mathbf{a}(\theta)s_l)^H\vec{x}_l] \end{aligned} \tag{A.3}$$

So that

$$\ln P(\mathbf{X}/\theta) = const + \frac{1}{\sigma^2}\sum_{l=1}^{J}[-\vec{x}_l^H\vec{x}_l - s_l^*\mathbf{a}(\theta)^H\mathbf{a}(\theta)s_l + \vec{x}_l^H\mathbf{a}(\theta)s_l + s_l^*\mathbf{a}(\theta)^H\vec{x}_l] \tag{A.4}$$

As indicated in [16, 20] Fisher information matrix can be written as

$$I(\theta) = -\mathbb{E}\left[\frac{\partial^2}{\partial\theta^2}\log P(\mathbf{X}/\theta)\right] \tag{A.5}$$

The first derivative of equation (A.4) w.r.t θ can be written as

$$\frac{\partial}{\partial\theta}\log P(\mathbf{X}/\theta) = \frac{1}{\sigma^2}\sum_{l=1}^{J}[-s_l^*\mathbf{a}'(\theta)^H\mathbf{a}(\theta)s_l - s_l^*\mathbf{a}(\theta)^H\mathbf{a}'(\theta)s_l + \vec{x}_l^H\mathbf{a}'(\theta)s_l + s_l^*\mathbf{a}'(\theta)^H\vec{x}_l] \tag{A.6}$$

Hence, second derivative will be

$$\begin{aligned}\frac{\partial^2}{\partial\theta^2}\log P(\mathbf{X}/\theta) = \frac{1}{\sigma^2}\sum_{l=1}^{J}[&-s_l^*\mathbf{a}''(\theta)^H\mathbf{a}(\theta)s_l - s_l^*\mathbf{a}'(\theta)^H\mathbf{a}'(\theta)s_l - s_l^*\mathbf{a}'(\theta)^H\mathbf{a}'(\theta)s_l \\ &- s_l^*\mathbf{a}(\theta)^H\mathbf{a}''(\theta)s_l + \vec{x}_l^H\mathbf{a}''(\theta)s_l + s_l^*\mathbf{a}''(\theta)^H\vec{x}_l]\end{aligned} \tag{A.7}$$

Taking expectation of equation (1) and then substitute in equation (A.7) will give the following

$$\begin{aligned}\frac{\partial^2}{\partial\theta^2}\log P(\mathbf{X}/\theta) = \frac{1}{\sigma^2}\sum_{l=1}^{J}[&-s_l^*\mathbf{a}''(\theta)^H\mathbf{a}(\theta)s_l - s_l^*\mathbf{a}'(\theta)^H\mathbf{a}'(\theta)s_l - s_l^*\mathbf{a}'(\theta)^H\mathbf{a}'(\theta)s_l \\ &- s_l^*\mathbf{a}(\theta)^H\mathbf{a}''(\theta)s_l + s_l^*\mathbf{a}(\theta)^H\mathbf{a}''(\theta)s_l + s_l^*\mathbf{a}''(\theta)^H\mathbf{a}(\theta)s_l]\end{aligned} \tag{A.8}$$

$$\begin{aligned}\frac{\partial^2}{\partial\theta^2}\log P(\mathbf{X}/\theta) &= \frac{1}{\sigma^2}\sum_{l=1}^{J} -2s_l^*\mathbf{a}'(\theta)^H\mathbf{a}'(\theta)s_l \\ &= \frac{-2J\mathbf{a}'(\theta)^H\mathbf{a}'(\theta)S_p}{\sigma^2}\end{aligned} \tag{A.9}$$

where S_p is the signal power and $\mathbf{a}(\theta)$ is the steering vector and can be defined as follows

$$\mathbf{a}(\theta) = \left[1,\ e^{-i2\pi F_c\frac{d\sin(\theta)}{C}}\ ,\dots,\ e^{-i2\pi F_c\frac{(M-1)d\sin(\theta)}{C}}\right]^T \tag{A.10}$$

where $K = \frac{2\pi}{\lambda_c}$ is the propagation constant.
Derivative of steering vector $\mathbf{a}(\theta)$ w.r.t (θ) can be written as follows

$$\mathbf{a}'(\theta) = -jKd\cos(\theta)[0\ ,\ \dots\ ,\ (m-1)e^{-i2\pi F_c\frac{(m-1)d\sin(\theta)}{C}}\ ,\ \dots\ ,\ (M-1)e^{-i2\pi F_c\frac{(M-1)d\sin(\theta)}{C}}]^T \tag{A.11}$$

$$\mathbf{a}'^H(\theta) = jKd\cos(\theta)[0\ ,\ \dots\ ,\ (m-1)e^{i2\pi F_c\frac{(M-1)d\sin(\theta)}{C}}\ ,\ \dots\ ,\ (M-1)e^{i2\pi F_c\frac{(M-1)d\sin(\theta)}{C}}]^T \tag{A.12}$$

Consequently, the term $\mathbf{a}'(\theta)^H\mathbf{a}'(\theta)$ can be written as follows

$$\mathbf{a}'(\theta)^H\mathbf{a}'(\theta) = (Kd\cos\theta)^2\sum_{m=1}^{M}(m-1)^2 \tag{A.13}$$

The result of substituting equation (A.13) into equation (A.9) will give the following

$$\frac{\partial^2}{\partial\theta^2}\log P(\mathbf{X}/\theta) = \frac{-2JS_p(Kd\cos(\theta))^2\sum_{m=1}^{M}(m-1)^2}{\sigma^2} \tag{A.14}$$

Hence

$$\mathbb{E}\left[\frac{\partial^2}{\partial\theta^2}\log P(\mathbf{X}/\theta)\right] = \frac{-2JS_p(Kd\cos(\theta))^2\sum_{m=1}^{M}(m-1)^2}{\sigma^2} \tag{A.15}$$

Hence, fisher information can be written as follows

$$\begin{aligned} I(\theta) = & -\mathbb{E}\left[\frac{\partial^2}{\partial\theta^2}\log P(\mathbf{X}/\theta)\right] \\ = & \frac{2JS_p(Kd\cos(\theta))^2\sum_{m=1}^{M}(m-1)^2}{\sigma^2} \end{aligned} \tag{A.16}$$

The SNR can be defined as

$$\alpha = \frac{S_p}{\sigma^2} \tag{A.17}$$

By substituting equation (A.17) into equation (A.16), the result can be written as

$$I(\theta) = 2J\alpha(Kd\cos(\theta))^2\sum_{m=1}^{M}(m-1)^2 \tag{A.18}$$

Equation (A.19) represents the relation between CRB and fisher information as indicated in [16, 20]

$$CRB \geq I^{-1} \tag{A.19}$$

Then CRB can be defined as follows

$$CRB \geq \frac{1}{2J\alpha(Kd\cos(\theta))^2\sum_{m=1}^{M}(m-1)^2} \tag{A.20}$$

References

[1] Rana N A 2016 *Cell* **92** 300–7272402
[2] Gentilho E, Scalassara P R and Abrão T 2020 *Journal of Signal Processing Systems* **92** 239–256
[3] Khmou Y, Safi S and Frikel M 2014 *Journal of Telecommunications and Information Technology*
[4] Abdullah A N and Abdul-Rahaim L A 2021 *Technology Reports of Kansai University* **63**
[5] Kratschmer G 2010 *Radiomonitoring and Radiolocation* **2011** 2011
[6] Poisel R A 2015 *Electronic warfare receivers and receiving systems* (Artech House)
[7] Denisowski P 2011 *presentation, Dept of Energy Spectrum Management Conference, Las Vegas*
[8] Ly P Q C 2013 *Fast and unambiguous direction finding for digital radar intercept receivers.* Ph.D. thesis
[9] Ko C B and Lee J H 2020 *Applied Sciences* **10** 2331
[10] Gross F B 2015 *Smart Antennas with MATLAB®* (McGraw-Hill Education)
[11] Godara L C 2004 *Smart antennas* (CRC press)
[12] Tang H 2014 Doa estimation based on music algorithm
[13] Sharma A and Mathur S 2016 *IETE Technical review* **33** 472–491
[14] Osman L, Sfar I and Gharsallah A 2012 *International Journal of Research and Reviews in Wireless Communications (IJRRWC) Vol* **2**
[15] Boustani B, Baghdad A, Sahel A, Ballouk A and Badr A 2018 *2018 4th International Conference on Optimization and Applications (ICOA)* (IEEE) pp 1–5
[16] Poor H V 2013 *An introduction to signal detection and estimation* (Springer Science & Business Media)
[17] Ko C B and Lee J H 2021 *Applied Sciences* **11** 467
[18] Krim H and Viberg M 1996 *IEEE signal processing magazine* **13** 67–94
[19] Stoica P and Nehorai A 1990 *IEEE Transactions on Acoustics, Speech, and Signal Processing* **38** 2140–2150
[20] Barkat M 2005 *Signal detection and estimation* (Artech House Publishers)
[21] Valdez K 2021 *Radio Direction Finding Implementing Music Algorithm with USRP Node Arrays* Ph.D. thesis The University of Texas at El Paso
[22] Anand A and Mukul M K 2016 *2016 IEEE International Conference on Recent Trends in Electronics, Information & Communication Technology (RTEICT)* (IEEE) pp 343–347
[23] Chowdary G P 2016 *International Journal of Review in Electronics and Communication Engineering* **4** 15–19

[24] Abdelbari A 2018 *Direction of arrival estimation of wideband RF sources* Ph.D. thesis Near East University Nicosia, Cyprus
[25] Shahid M U, Nauman M, Haider D and Imran Y 2017 *2017 International Conference on Infocom Technologies and Unmanned Systems (Trends and Future Directions)(ICTUS)* (IEEE) pp 451–454
[26] Ali S S, Liu C, Liu J, Jin M, Yoo S J and Kim J M 2017 *2017 International Conference on Information and Communication Technology Convergence (ICTC)* (IEEE) pp 480–485
[27] Devendra M and Manjunathachari K 2015 *2015 International Conference on Signal Processing and Communication Engineering Systems* (IEEE) pp 309–313
[28] Shan T J, Wax M and Kailath T 1985 *IEEE Transactions on Acoustics, Speech, and Signal Processing* **33** 806–811
[29] Goverdovsky V, Yates D C, Willerton M, Papavassiliou C and Yeatman E 2016 *IEEE Transactions on Instrumentation and Measurement* **65** 1577–1584
[30] Borkar A N 2019 *2019 3rd International conference on Electronics, Communication and Aerospace Technology (ICECA)* (IEEE) pp 1355–1359
[31] Shirvani-Moghaddam S and Almasi-Monfared S 2011 *International Journal on Communications Antenna and Propagation (IRECAP)* **1**
[32] Monzingo R A and Miller T W 2004 *Introduction to adaptive arrays* (Scitech publishing)